ChemPubSoc Europe

DOI: 10.1002/ejoc.201700566

EurJOC European Journal of Organic Chemistry

Full Paper

Drug Delivery

Monitoring Fluorinated Dendrimer-Based Self-Assembled Drug-Delivery Systems with ^{19}F Magnetic Resonance

Xin Liu,[a] Yaping Yuan,[b] Shaowei Bo,[a] Yu Li,[a] Zhigang Yang,[a] Xin Zhou,[b] Shizhen Chen,*[b] and Zhong-Xing Jiang*[a,c]

Abstract: Monitoring a drug-delivery system with an imaging modality is of great importance for detailed understanding of drug-delivery processes and for achieving optimal therapeutic effects. Here, novel fluorinated self-assembled dendrimers with a single ^{19}F NMR signal were conveniently synthesized on multigram scales, and ^{19}F magnetic resonance, including spectroscopy (^{19}F NMR) and imaging (^{19}F MRI), was used to monitor the fluorinated dendrimer-based self-assembled drug-delivery systems. It was found that ^{19}F NMR and ^{19}F MRI were convenient and sensitive tools to monitor the self-assembly and drug-loading processes and to detect weak interactions between the drug and the drug-delivery vehicle because changes in the self-assembly profile sensitively induced corresponding ^{19}F magnetic resonance responses.

Introduction

Self-assembly is an important phenomenon that plays a crucial role in many drug-delivery systems.[1] For example, liposome- and micelle-based drug-delivery systems are mainly based on the self-assembly of amphiphiles to encapsulate, stabilize, and deliver drugs. Therefore, novel strategies to study self-assembly are of great importance for the design of novel self-assembled systems that can be used to monitor the drug-delivery process and to optimize drug therapy.

^{19}F Magnetic resonance imaging (^{19}F MRI) and ^{19}F nuclear magnetic resonance (^{19}F NMR) spectroscopy are powerful tools in monitoring chemical and biochemical reactions,[2] drug–target interactions,[3] protein dynamics and interactions,[4] nucleic-acid recognition,[5] and biodistribution of targets.[6] Besides the inherent advantages of magnetic resonance, for example, no tissue depth limit or ionizing radiation, ^{19}F MRI and ^{19}F NMR spectroscopy provide not only quantitative images and spectra with high sensitivity and negligible background, but also sensitive responses to microenvironments.[7] These features make ^{19}F MRI/NMR appropriate tools for monitoring self-assembly in drug-delivery systems.

Self-assembled fluorinated amphiphiles are promising drug-delivery vehicles, because the in vivo drug-delivery process can be conveniently monitored by ^{19}F MRI and ^{19}F NMR, which may facilitate personalized drug therapy.[8] However, as far as we know, there are only a few reports on the ^{19}F-MRI- and ^{19}F-NMR-monitored self-assembly of fluorinated amphiphiles.[6d,9] Therefore, it is of great importance to develop novel self-assembled fluorinated amphiphiles as ^{19}F-MRI- and ^{19}F-NMR-traceable drug-delivery vehicles and to perform comprehensive ^{19}F MRI and ^{19}F NMR studies on their self-assembly behaviors and drug–vehicle interactions.

The design of fluorinated self-assembled dendrimers is crucial for efficient encapsulation and delivery of drugs as well as for sensitive detection of the process by ^{19}F MRI and ^{19}F NMR spectroscopy. Fluorinated Janus dendrimers **1b** and **2b** were then designed as self-assembled amphiphiles in which weak interactions, that is, π–π stacking and hydrophobic effects of the phenyl and trifluoromethyl groups, were employed as the driving force for self-assembly (Figure 1). In amphiphiles **1b** and **2b**, each moiety plays a certain role, that is, the fluorinated benzyl group serves as a hydrophobic head, monodispersed oligoethylene glycol units act as hydrophilic tails, and 12 symmetric fluorine atoms together serve as a sensitive ^{19}F MRI/NMR signal emitter without chemical-shift artefacts.[10] A thiol group was introduced in **1a** and **2a** for further modification, such as their attachment to gold nanoparticles, biomolecules, and drugs. It is noteworthy that the hydrophilic–hydrophobic balance can be monitored by the length of the monodisperse oligoethylene glycol units and the number of phenyl groups. Besides tuning the hydrophilic–hydrophobic balance, the two additional phenyl groups in **1a**–**c** were also used to evaluate their hydrophobic effects and π–π interactions in the self-assembly drug-delivery system.

[a] *Hubei Province Engineering and Technology Research Center for fluorinated Pharmaceuticals, School of Pharmaceutical Sciences, Wuhan University, Wuhan 430071, China*
E-mail: zxjiang@whu.edu.cn
http://pharmacy.whu.edu.cn
[b] *State Key Laboratory for Magnetic Resonance and Atomic and Molecular Physics, Wuhan Institute of Physics and Mathematics, Chinese Academy of Sciences, Wuhan 430071, China*
E-mail: chenshizhen@wipm.ac.cn
http://www.wipm.cas.cn/
[c] *State Key Laboratory for Modification of Chemical Fibers and Polymer Materials, Dong Hua University, Shanghai 201620, China*
Supporting information and ORCID(s) from the author(s) for this article are available on the WWW under https://doi.org/10.1002/ejoc.201700566.

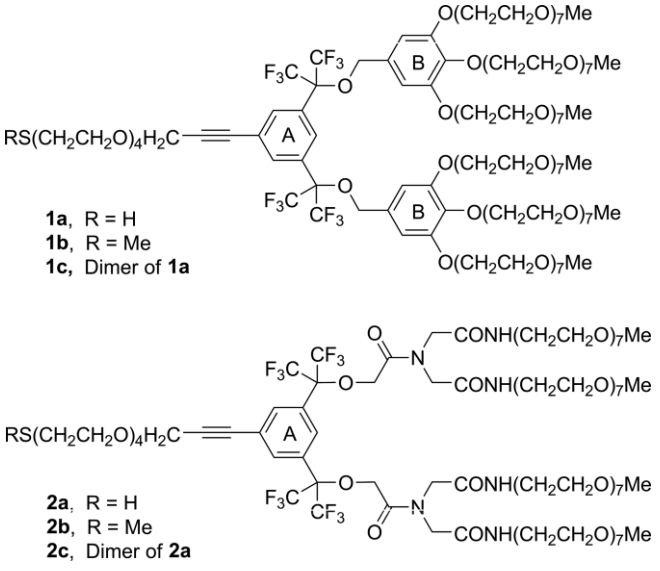

Figure 1. Structures of fluorinated amphiphiles **1a**–**c** and **2a**–**c**.

Results and Discussion

These fluorinated amphiphiles were synthesized in a convergent way with high efficacy (Scheme 1). Strategies previously developed in this group were applied to manipulate the monodisperse oligoethylene glycols.[6d,11] Sonogashira coupling and Williamson ether synthesis were employed to conjugate the hydrophilic tails to the hydrophobic head in high yields. Disulfide **1c** and **2c** were then directly transformed into **1b** and **2b**, respectively, because thiols **1a** and **2a** were very unstable in air. Finally, target fluorinated amphiphiles **1b** and **2b** were synthesized over 11 steps on multigram scales. As expected, each fluorinated amphiphile gives only 1 ^{19}F NMR signal from its 12 symmetric fluorine atoms (Figure 2), which dramatically increases the ^{19}F NMR/MRI sensitivity of these amphiphiles.

The self-assembly of fluorinated amphiphiles **1b** and **2b** was then studied by ^{19}F NMR spectroscopy. First, the solvent-dependent ^{19}F NMR spectra show line broadening and chemical-shift changes upon increasing the water content of the solvent (Figure 3a, c), which is a result of increased molecular interactions due to self-assembly of **1b** and **2b**. Second, the solvent isotope effect indicates that changes in the chemical shift ($\Delta\delta$) are mainly induced by self-assembly and that the trifluoromethyl groups have limited exposure to water (Figure S1 in the Supporting Information).[4] Third, the temperature-dependent ^{19}F NMR spectra show line broadening at elevated temperatures as a result of faster molecular tumbling (Figure S1). Finally, the self-assembly of **1b** and **2b** was further confirmed by concentration-dependent ^{19}F NMR spectroscopy, for which a self-assembly-induced $\Delta\delta$ break point corresponds to the critical micelle concentration (CMC, Figure 2b, d). The CMC of **1b** in D_2O was calculated from the concentration-dependent ^{19}F NMR and ^{1}H NMR spectra as 4.45 and 2.42 mM, respectively (Figure 3e, f; the two symmetric protons on ring A were selected for ^{1}H NMR spectroscopy). The difference in the CMC values from the ^{19}F NMR and ^{1}H NMR spectra probably originates from the different microenvironments of the fluorine and hydrogen

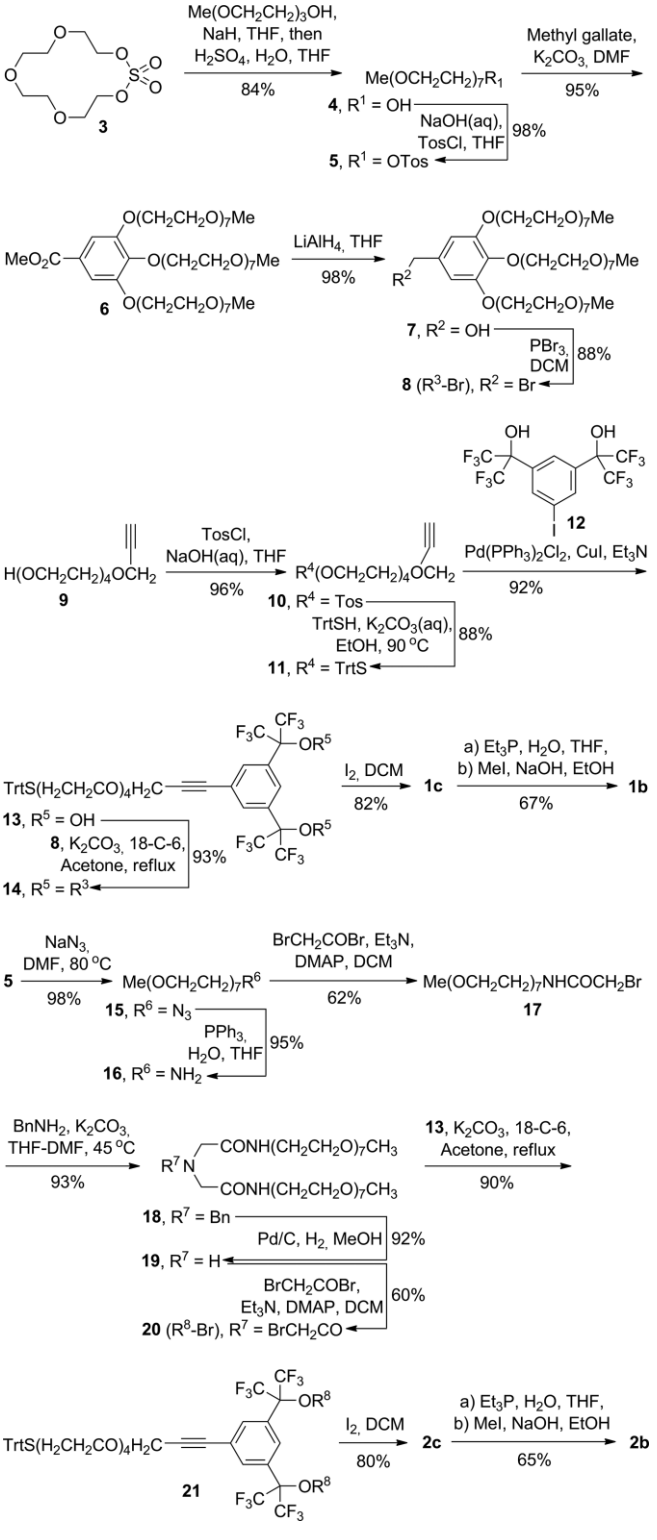

Scheme 1. Synthesis of fluorinated amphiphiles **1a**–**c** and **2a**–**c**. Tos = tosyl, DCM = dichloromethane, Trt = trityl (triphenylmethyl), DMAP = 4-(dimethylamino)pyridine.

atoms. Amphiphile **2b** exhibits a higher CMC of 7.35 mM, as determined by ^{19}F NMR spectroscopy, as a result of its higher hydrophilicity (Figure S2).

Structurally, relative to **2b**, the two phenyl groups in **1b** promote self-assembly through hydrophobic effects and π–π inter-

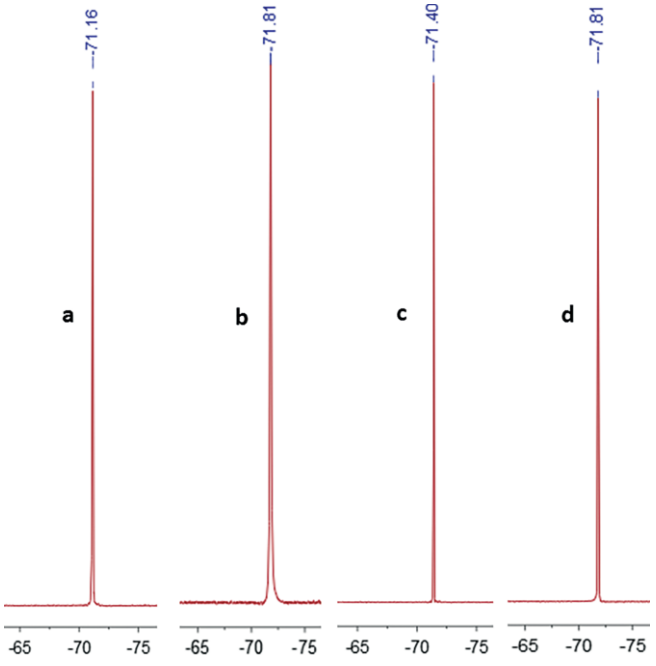

Figure 2. ^{19}F NMR spectra of **1b** in (a) MeOH and (b) H_2O, and ^{19}F NMR spectra of **2b** in (c) MeOH and (d) H_2O.

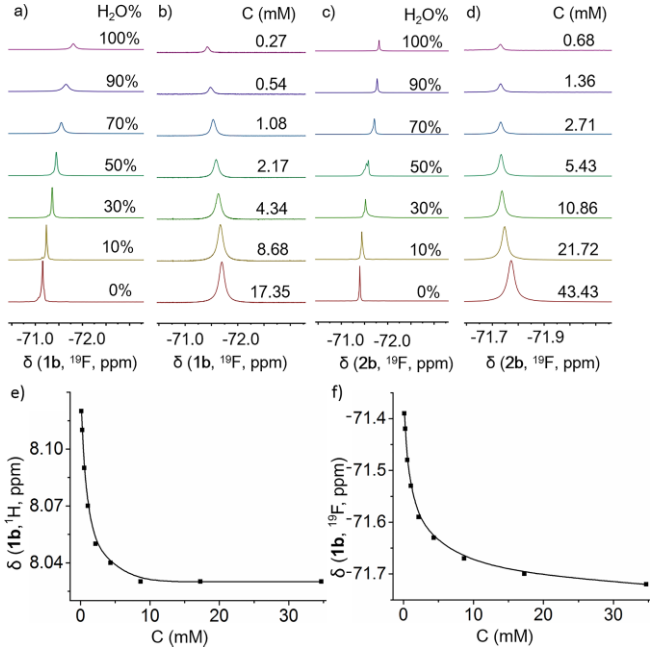

Figure 3. Solvent-dependent (17.36 mM, 25 °C) ^{19}F NMR spectra of (a) **1b** and (c) **2b** and concentration-dependent (D_2O, 25 °C) ^{19}F NMR spectra of (b) **1b** and (d) **2b**; CMC of **1b**, as determined by (e) ^{1}H NMR and (f) ^{19}F NMR spectroscopy.

actions. Therefore, **1b** is more sensitive than **2b** to changes in the microenvironment, such as solvent, concentration, and temperature. Interestingly, the difference can be sensitively detected by the $\Delta\delta$ value determined by ^{19}F NMR spectroscopy. Besides the fact that the $\Delta\delta$ value of **2b** ($\Delta\delta$ = 0.04 ppm) is much smaller than that of **1b** ($\Delta\delta$ = 0.28 ppm), as determined by the concentration-dependent ^{19}F NMR spectra, a smaller $\Delta\delta$ value in the solvent-dependent ^{19}F NMR spectra was also found for **2b** (solve changed from 100 % MeOH to 100 % H_2O: **1b** $\Delta\delta$ = 0.65 ppm, **2b** $\Delta\delta$ = 0.41 ppm; solve changed from 100 % MeOH to 100 % D_2O: **1b** $\Delta\delta$ = 0.56 ppm, **2b** $\Delta\delta$ = 0.34 ppm). The difference was further confirmed by dynamic light scattering (DLS), which indicated that **1b** aggregated into spherical nanoparticles with a diameter of 6.3 nm, whereas the size of **2b** was too small to be measured by DLS. On the basis of the above observation, it is clear that ^{19}F NMR spectroscopy is a sensitive and convenient tool to monitor self-assembly processes, to detect changes in the microenvironment, and to reveal structural differences in amphiphiles.

To study drug–amphiphile interactions in micelle- and liposome-based drug-delivery systems, ^{19}F NMR spectroscopy was employed to monitor the co-self-assembly of **1b** and **2b** with drugs. A total of 15 small molecules with structural diversity, such as (*R*)-carvone (**C**), cholesterol (**O**), the anesthetic propofol (**I**), and the anticancer drug doxorubicin (**N**), were selected as representative "drugs" (Figure 4a). Relative to aqueous solutions of **1b** and **2b**, the co-self-assembled solutions of **1b** and **2b** with "drugs" showed very slight changes in the ^{19}F NMR chemical shift, $\Delta\delta$ < 0.05 ppm. This phenomenon promoted us to study the ^{1}H NOESY spectra of **1b** and **2b** in the presence of **G** in D_2O to detect the occurrence of co-self-assembly. Indeed, NOE effects were found between **1b** and **G** and between **2b** and **G**, which indicated that the amphiphile and drug were close to each other as a result of co-self-assembly (Figure 4b, c). However, the co-self-assembly had no effect on the exposure of fluorine to water, because fluorine–water interactions are a major promoter of $\Delta\delta$ (Figure 3). Therefore, the ^{19}F NMR $\Delta\delta$ value is actually not a sensitive parameter to detect structural differences in the encapsulated "drugs". However, marked changes in the signal intensity (ΔSI), which is another observable parameter of the "drug"–amphiphile interactions in co-self-assembly systems, were detected by ^{19}F NMR spectroscopy (Figure 4e). The patterns of the ^{19}F NMR ΔSI values for the **1b** and **2b** co-self-assembly systems are quite different. For systems with **2b**, "drugs" **A**–**O** all decreased the ^{19}F NMR SI value, and 1-octanol (**A**) gave a maximum ΔSI value of –33 %. The all-negative ΔSI value suggests that **2b** and "drugs" co-self-assemble through similar modes of interactions. For systems with **1b**, the "drugs" gave more complicated ^{19}F NMR ΔSI values. "Drugs" **L**, **N**, and **K** decreased the ^{19}F NMR SI value, and others increased the ^{19}F NMR SI values. This phenomenon is a result of more complex modes of interaction and self-assembly between **1b** and **A**–**O** owing to the presence of two additional phenyl groups in **1b**. The ^{1}H NOESY spectra of **1b** and **2b** in the presence of **G** (Figure 4b, c) also indicate that the interaction between **1b** and **G** is much stronger than that between **2b** and **G**. Therefore, the drug–amphiphile interaction can be visualized by the ^{19}F NMR ΔSI value, which is sensitive to the mode and strength of the interaction between the drug and amphiphile used in the drug-delivery system.

The co-self-assembly systems of amphiphiles **1b** and **2b** with selected "drugs" **A**, **C**, **H**, **K**, and **N** were then studied with transverse relaxation time (T_2)-weighted ^{19}F MRI on a 9.4 T scanner

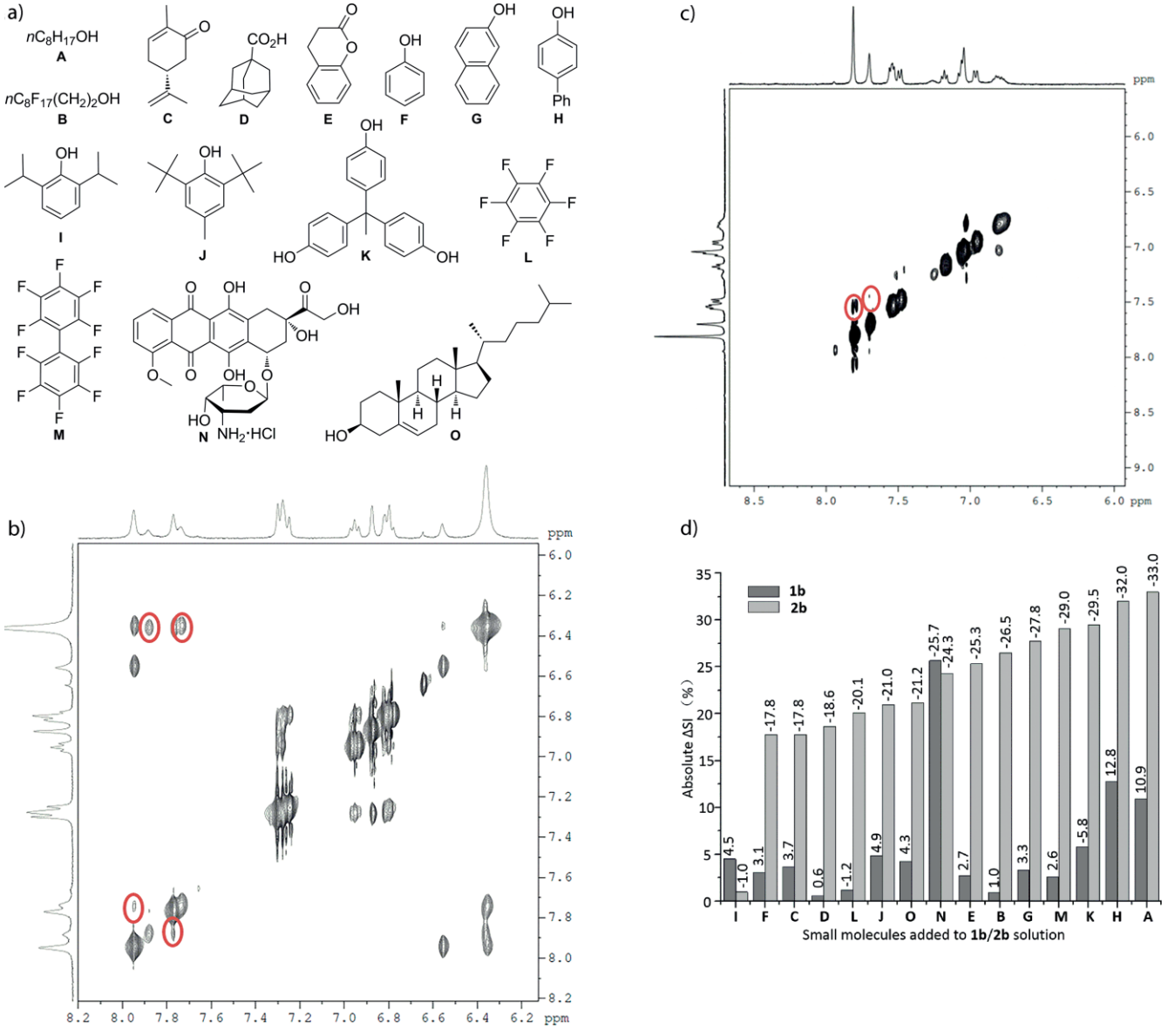

Figure 4. Co-self-assembly of fluorinated amphiphiles **1b** and **2b** with "drugs" **A**–**O**. (a) Structures of selected "drugs". ^{1}H NOESY spectra of (b) **1b** and (c) **2b** in the presence of **G** in D_2O, and (d) the ^{19}F NMR ΔSI values of co-self-assembly solutions. Amphiphile **1b** or **2b** (8.68 mM) was mixed with each "drug" in a 1:1 ratio, and the mixture was stirred for 12 h before ^{19}F NMR/MRI measurements. ΔSI = [SI(co-assembly) – SI(**1b**/**2b**)]/SI(**1b**/**2b**) × 100 %.

(Figure 5). First, solvent-dependent ^{19}F MRI of **1b** and **2b** showed a much higher signal-to-noise ratio (S/N) in methanol than in water because the self-assembly in water dramatically shortens T_2 and reduces their diffusion, which is consistent with our previous results.[10a] It is noteworthy that the structural difference between **1b** and **2b** can be visualized by ^{19}F MRI upon changing the solvent from methanol to water. In the solvent-dependent experiments, the T_2, S/N, and diffusion coefficient (*D*) of hydrophobic **1b** were significantly reduced by 85, 81, and 37 %, respectively, whereas limited reductions were found for hydrophilic **2b**. Second, additive-dependent ^{19}F MRI of **1b** and **2b** showed considerable S/N changes in the presence of the "drug". The S/N of **1b** was dramatically increased in the presence of 1-octanol (**A**), (*R*)-carvone (**C**), and 4-phenylphenol (**H**) by 35, 38, and 31 %, respectively, whereas 4,4′,4″-(ethane-1,1,1-triyl)triphenol (**K**) and doxorubicin (**N**) severely decreased the S/N by 48 and 40 %, respectively (Figure 5a). It is important to point out that this trend is consistent with the trend of their T_2 and additive-dependent ^{19}F NMR ΔSI values. In contrast, the presence of the "drug" had a much smaller influence on the S/N for **2b** (up to 19 %, Figure 5b), which is probably due to the facts that **2b** has higher hydrophilicity than **1b**, the "drug"–**2b** interactions are weaker than the "drug"–**1b** interactions, and **2b** forms much smaller co-self-assembled nanoparticles than **1b**. Thus, ^{19}F MRI can not only provide images of the co-self-assembled amphiphile–drug systems for drug tracking and dosing optimization, but it can also show amphiphile–drug interactions by revealing structural differences among the drugs, which should be very useful for monitoring drug-loading and drug-release processes.

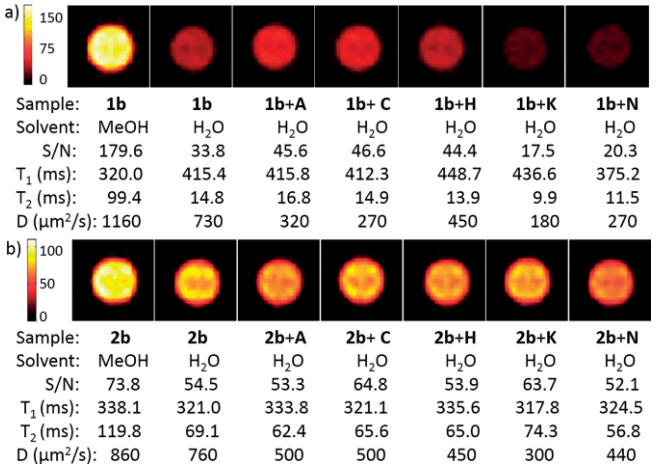

Sample:	1b	1b	1b+A	1b+ C	1b+H	1b+K	1b+N
Solvent:	MeOH	H_2O	H_2O	H_2O	H_2O	H_2O	H_2O
S/N:	179.6	33.8	45.6	46.6	44.4	17.5	20.3
T_1 (ms):	320.0	415.4	415.8	412.3	448.7	436.6	375.2
T_2 (ms):	99.4	14.8	16.8	14.9	13.9	9.9	11.5
D (μm²/s):	1160	730	320	270	450	180	270

Sample:	2b	2b	2b+A	2b+ C	2b+H	2b+K	2b+N
Solvent:	MeOH	H_2O	H_2O	H_2O	H_2O	H_2O	H_2O
S/N:	73.8	54.5	53.3	64.8	53.9	63.7	52.1
T_1 (ms):	338.1	321.0	333.8	321.1	335.6	317.8	324.5
T_2 (ms):	119.8	69.1	62.4	65.6	65.0	74.3	56.8
D (μm²/s):	860	760	500	500	450	300	440

Figure 5. Solvent-dependent and additive-dependent ^{19}F MRI of **1b** and **2b** and their co-self-assembled mixtures with "drugs" **A**, **C**, **H**, **K**, and **N**. T_1, T_2, and D were measured simultaneously with ^{19}F MRI.

Finally, fluorinated amphiphiles **1a** and **2a** were employed to investigate their self-assembly on gold nanoparticles (GNPs). After modifying GNPs with in situ generated thiols **1a** and **2a** from corresponding disulfides **1c** and **2c**, the GNPs were covered with a highly ordered layer of **1a** or **2a**, because monodisperse oligoethylene glycol units were used as anchors on the GNPs. DLS indicated the average diameter of the GNPs was expanded from 20 to 24 nm after **1a** modification. However, there was only a slight size change, ≈0.5 nm in diameter, in the GNPs modified with **2a**. The difference is probably because **1a** has a larger molecular size than **2a**, and therefore, there is a denser layer of monodisperse oligoethylene glycol units on the **2a**-modified GNPs. Because the order and dense arrangement of **1a** and **2a** on the GNPs would enhance intermolecular π–π stacking and hydrophobic interactions and because the Au–S bond would further reduce the molecular movement of **1a** and **2a**, molecular tumbling of **1a** and **2a** on the GNPs was severely reduced. It was reported that restricting the mobility of fluorine atoms on GNPs dramatically broadened the ^{19}F NMR signal or even quenched the ^{19}F NMR signal.[12] Therefore, very weak singlets in the ^{19}F NMR spectra of the **1a**- and **2a**-modified GNPs are detected, which indicates that **1a** and **2a** are homogeneously distributed on the GNPs and that all of the fluorine atoms have similar environments. For **1a**- and **2a**-modified GNPs solutions at the same fluorine concentration, the lower ^{19}F NMR S/N of the **1a**-modified GNPs is also an indication that additional π–π stacking and hydrophobic interactions from the B rings further restrict the mobility of the fluorine atoms on the GNPs. However, the ^{19}F NMR signal is too weak to obtain a decent image from ^{19}F MRI within a reasonable scanning time at this concentration. So, the molecular movement is also an important factor in the design of ^{19}F NMR/MRI-sensitive drug-delivery systems, especially for nanoparticle-based systems. Thus, ^{19}F NMR spectroscopy is able to detect weak interactions in self-assembly even on GNPs (Figure 6).

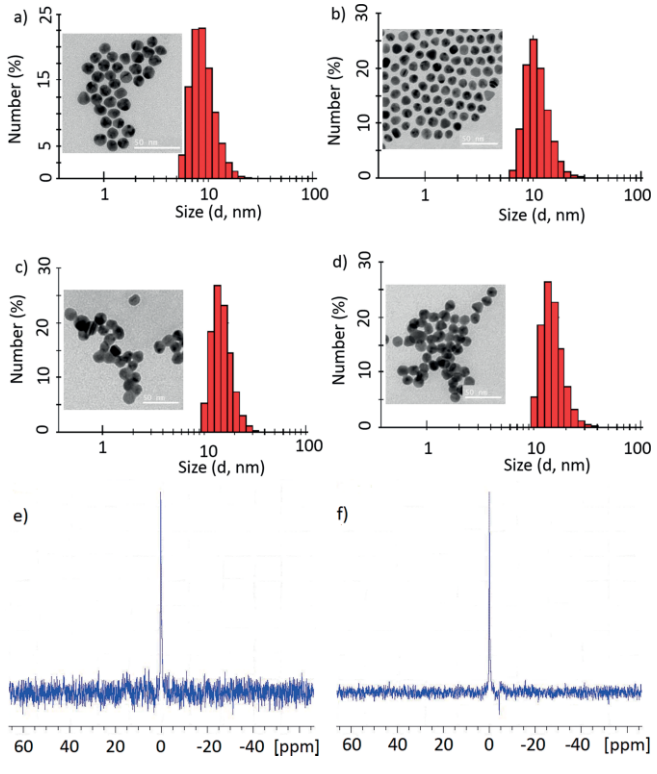

Figure 6. (a,c) DLS of **1a**-modified GNPs with TEM images of free GNPs in the inset of panel a and aggregated GNPs in the inset of panel c, (b,d) DLS of **2a**-modified GNPs with TEM images free GNPs in the inset of panel b and aggregated GNPs in the inset of panel d, and (e,f) ^{19}F NMR spectra of **1a**-modified GNPs and **2a**-modified GNPs. The scale bars for the TEM images are 50 nm.

Conclusions

In conclusion, ^{19}F NMR/MRI are appropriate tools for monitoring self-assembled drug-delivery systems. Besides images and spectra, the plentiful parameters of ^{19}F NMR/MRI, such as chemical shift, which is sensitive to solvent; signal intensity, which is sensitive to the structure of the encapsulated drug; and relaxation time, which is sensitive to molecular tumbling, provide insightful understanding about the self-assembly process, drug–delivery vehicle interactions, drug structural features, and so on. Fluorinated self-assembled amphiphiles are promising ^{19}F NMR/MRI-traceable drug-delivery vehicles for in vivo tracing and quantifying drugs and detecting drug microenvironments and weak interactions and, therefore, developing ^{19}F NMR/MRI-guided drug therapy. Although this study illustrated the feasibility of using ^{19}F NMR/MRI to monitor drug-delivery systems sensitively and to provide principles for rational ^{19}F NMR/MRI-sensitive drug-delivery vehicles, novel fluorinated drug-delivery vehicles based on this work to improve drug loading ability, targeted delivery, and ^{19}F NMR/MRI sensitivity are necessary to translate these in vitro studied into in vivo ^{19}F NMR/MRI-guided drug therapy. Currently, these works are actively ongoing in this laboratory.

Experimental Section

Synthesis of 4: At 0 °C, under an atmosphere of argon, a solution of triethylene glycol monomethyl ether (29.90 g, 182.10 mmol) in

THF (150 mL) was added to a suspension of NaH (60 % dispersed in mineral oil, 10.93 g, 273.15 mmol in 500 mL of THF). The mixture was stirred for 30 min, and a solution of **3**[11] (70 g, 273.15 mmol) in THF (250 mL) was added. The resulting mixture was stirred overnight at room temperature. Then, water (4.92 mL, 273.15 mmol) was added to the mixture, and H_2SO_4 was added to adjust the pH to about 3. The resulting mixture was stirred overnight at room temperature. The reaction was quenched with saturated Na_2CO_3 to adjust the pH to about 7. After removal of the solvent under vacuum, the solution was washed with water and extracted with CH_2Cl_2 (4 × 500 mL). The organic layers were combined, and the solution was concentrated under vacuum. The residue was purified by column chromatography (MeOH/CH_2Cl_2 = 3:100) to give **4** (52.07 g, 84 %) as a clear oil. ^{1}H NMR (400 MHz, $CDCl_3$): δ = 3.38 (s, 3 H), 3.52–3.79 (m, 28 H) ppm.

Synthesis of 5: To a stirring solution of ethanol **4** (52.07 g, 152.96 mmol) in THF (500 mL) was added aqueous sodium hydroxide (24.47 g of NaOH in 73.41 mL of water). After stirring for 10 min and cooling to 0 °C, *p*-toluenesulfonyl chloride (58.32 g, 305.93 mmol) in THF (200 mL) was slowly added to the mixture. After the addition was complete, the mixture was warmed to room temperature and was stirred overnight. The resulting mixture was extracted with EtOAc (3 × 400 mL). The organic layers were combined, and the solution was concentrated under vacuum. The residue was purified by column chromatography (EtOAc/petroleum ether = 2:1) to give **5** as a colorless oil (74.14 g, 98 %). ^{1}H NMR (400 MHz, $CDCl_3$): δ = 2.45 (s, 3 H), 3.38 (s, 3 H), 3.53–3.72 (m, 26 H), 4.16 (t, *J* = 4.0 Hz, 2 H), 7.35 (d, *J* = 8.0 Hz, 2 H), 7.80 (d, *J* = 8.0 Hz, 2 H) ppm.

Synthesis of 6: Under an argon atmosphere, a mixture of methyl gallate (6.52 g, 35.4 mmol) and K_2CO_3 (44.03 g, 318.6 mmol) in dry DMF (150 mL) was stirred at 70 °C for 30 min, and then a solution of **5** (61.28 g, 123.90 mmol) in dry DMF (150 mL) was added. The resulting mixture was then stirred at 70 °C overnight. After removing DMF by vacuum distillation, the reaction was quenched with water (200 mL) and was extracted with CH_2Cl_2 (4 × 250 mL). The organic layers were combined, and the solution was concentrated under vacuum. The residue was purified by column chromatography (MeOH/CH_2Cl_2 = 1:50) to give **6** as a colorless oil (38.72 g, 95 %). ^{1}H NMR (400 MHz, $CDCl_3$): δ = 3.38 (s, 9 H), 3.51–3.91 (m, 83 H), 4.15–4.24 (m, 6 H), 7.29 (s, 2 H) ppm. ^{13}C NMR (100 MHz, $CDCl_3$): δ = 25.5, 52.1, 58.9, 67.8, 68.7, 69.5, 70.3, 70.4, 70.5, 70.6, 70.7, 71.8, 72.3, 108.7, 124.8, 142.3, 152.1, 166.4 ppm. HRMS (ESI): calcd. for $C_{53}H_{102}NO_{26}^+$ [M + NH_4]$^+$ 1168.6685; found 1168.6692.

Synthesis of 7: Under an argon atmosphere, to a stirring suspension of $LiAlH_4$ (3.83 g, 100.89 mmol) in dry THF (100 mL) at 0 °C was added a solution of **6** (38.72 g, 33.63 mmol) in THF (50 mL). The mixture was stirred at room temperature overnight. The reaction was quenched at 0 °C with 30 % NaOH/H_2O [$LiAlH_4$/30 % NaOH/H_2O = 1:2:3 (*w*/*v*/*v*)]. The organic layers were combined, and the solution was dried with anhydrous Na_2SO_4, filtered, and concentrated under reduced pressure. The resulting residue was purified by column chromatography (MeOH/CH_2Cl_2 = 1:50) to give **7** as a clear oil (37.02 g, 98 %). ^{1}H NMR (400 MHz, $CDCl_3$): δ = 3.38 (s, 9 H), 3.51–3.89 (m, 81 H), 4.09–4.21 (m, 6 H), 4.57 (d, *J* = 8.0 Hz, 2 H), 6.63 (s, 2 H) ppm. ^{13}C NMR (100 MHz, $CDCl_3$): δ = 58.8, 64.3, 68.5, 69.6, 70.3, 70.4, 70.6, 71.7, 72.1, 105.9, 137.0, 137.3, 152.3 ppm. MS (MALDI-TOF): calcd. 1145.6 [M + Na]$^+$; found 1145.6.

Synthesis of 8: Under an argon atmosphere, to a stirring solution of alcohol **7** (30.60 g, 27.24 mmol) in dry CH_2Cl_2 (150 mL) was slowly added PBr_3 (7.76 mL, 81.72 mmol) at 0 °C, and the resulting mixture was stirred at room temperature for 5 h. The reaction was quenched with EtOH, and the mixture was extracted with EtOAc (3 × 150 mL). The organic layers were combined, and the solution was dried with anhydrous $MgSO_4$, filtered, and concentrated to dryness. The residue was purified by column chromatography (MeOH/CH_2Cl_2 = 1:50) to give bromide **8** as a clear oil (28.43 g, 86 %). ^{1}H NMR (400 MHz, $CDCl_3$): δ = 3.38 (s, 9 H), 3.52–3.89 (m, 80 H), 4.10–4.19 (m, 6 H), 4.43 (d, *J* = 4.0 Hz, 2 H), 6.64 (d, *J* = 8.0 Hz, 2 H) ppm. ^{13}C NMR (100 MHz, $CDCl_3$): δ = 34.0, 58.8, 68.7, 69.5, 70.3, 70.4, 70.6, 71.7, 72.1, 108.5, 132.8, 138.3, 152.4 ppm. HRMS (ESI): calcd. for $C_{52}H_{99}BrO_{24}^{2+}$ [M + 2H]$^{2+}$ 593.2850; found 593.2827.

Synthesis of 10: Compound **10** was prepared by following the same procedure as that outlined for **5** from alcohol **4** as a clear oil (30.02 g, 96 %). ^{1}H NMR (400 MHz, $CDCl_3$): δ = 2.39–2.49 (m, 4 H), 3.59 (s, 4 H), 3.62–3.72 (m, 10 H), 4.16 (t, *J* = 4.0 Hz, 2 H), 4.20 (d, *J* = 2.4 Hz, 2 H), 7.35 (d, *J* = 8.0 Hz, 2 H), 7.80 (d, *J* = 8.0 Hz, 2 H) ppm.

Synthesis of 11: A mixture of **10** (30.02 g, 77.68 mmol), TrtSH (27.91 g, 100.98 mmol), and K_2CO_3 (21.47 g, 155.36 mmol) in H_2O/EtOH (1:1, 300 mL) was heated at reflux for 18 h. The resulting mixture was extracted with EtOAc (3 × 250 mL). The organic layers were combined, and the solution was concentrated under vacuum. The residue was purified by column chromatography (EtOAc/petroleum ether = 1:5) to give **11** as a pale-yellow oil (33.54 g, 88 %). ^{1}H NMR (400 MHz, $CDCl_3$): δ = 2.40–2.46 (m, 3 H), 3.29 (t, *J* = 8.0 Hz, 2 H), 3.42–3.46 (m, 2 H), 3.54–3.58 (m, 2 H), 3.61–3.69 (m, 9 H), 4.18 (d, *J* = 2.4 Hz, 2 H), 7.17–7.27 (m, 6 H), 7.28–7.33 (m, 2 H), 7.38–7.46 (m, 7 H) ppm. ^{13}C NMR (100 MHz, $CDCl_3$): δ = 31.8, 58.4, 66.6, 69.1, 69.6, 70.2, 70.4, 70.5, 70.6, 75.0, 79.8, 126.8, 128.0, 129.7, 144.9 ppm. HRMS (ESI): calcd. for $C_{30}H_{34}NaO_4S^+$ [M + Na]$^+$ 513.2070; found 513.2066.

Synthesis of 13: Under an argon atmosphere, to a mixture of alcohol **12**[10] (30.54 g, 56.97 mmol), $Pd(PPh_3)_2Cl_2$ (2.00 g, 2.85 mmol), and CuI (0.43 g, 2.28 mmol) in dry Et_3N (250 mL) was added a solution of **11** (33.54 g, 68.36 mmol) in dry Et_3N (25 mL) at room temperature, and the resulting mixture was stirred at this temperature overnight. The mixture was extracted with EtOAc (2 × 250 mL). The organic layers were combined, and the solution was dried with anhydrous $MgSO_4$, filtered, and concentrated under vacuum. The residue was purified by column chromatography (EtOAc/petroleum ether = 1:7) to give alcohol **13** as a clear oil (47.11 g, 92 %). ^{1}H NMR (400 MHz, $CDCl_3$): δ = 2.43 (t, *J* = 8.0 Hz, 2 H), 3.26 (t, *J* = 8.0 Hz, 2 H), 3.36–3.46 (m, 2 H), 3.49–3.57 (m, 2 H), 3.60–3.70 (m, 6 H), 3.71–3.77 (m, 2 H), 4.36 (s, 2 H), 5.65 (s, 2 H), 7.16–7.26 (m, 6 H), 7.27–7.30 (m, 2 H), 7.38–7.7.46 (m, 7 H), 7.87 (s, 2 H), 8.12 (s, 1 H) ppm. ^{13}C NMR (100 MHz, $CDCl_3$): δ = 17.7, 31.4, 58.4, 59.0, 66.7, 69.3, 69.6, 69.9, 70.2, 70.4, 85.1, 86.4, 122.7 (q, *J* = 286 Hz), 123.6, 125.8, 126.7, 128.0, 129.6, 131.8, 131.9, 144.8 ppm. ^{19}F NMR (376 MHz, $CDCl_3$): δ = –78.64 ppm. HRMS (ESI): calcd. for $C_{42}H_{38}F_{12}NaO_6S^+$ [M + Na]$^+$ 921.2090; found 921.2098.

Synthesis of 14: Under an argon atmosphere, a mixture of bromide **8** (27.79 g, 23.43 mmol), alcohol **13** (7.80 g, 8.68 mmol), dry K_2CO_3 (3.60 g, 26.03 mmol), and 18-crown-6 (0.46 g, 1.74 mmol) in anhydrous acetone (100 mL) was heated at reflux for 36 h. Then, the mixture was cooled to room temperature. The reaction was quenched with water (200 mL), and the resulting mixture was extracted with EtOAc (5 × 200 mL). The organic layers were combined, and the solution was dried with anhydrous $MgSO_4$, filtered, and concentrated under vacuum. The residue was purified by column chromatography (MeOH/CH_2Cl_2 = 1:25) to give **14** as a clear oil (25.10 g, 93 %). ^{1}H NMR (400 MHz, $CDCl_3$): δ = 2.44 (t, *J* = 8.0 Hz, 2 H), 3.39 (s, 18 H), 3.52–3.60 (m, 15 H), 3.61–3.77 (m, 143 H), 3.77–3.88 (m, 13 H), 4.10 (t, *J* = 8.0 Hz, 8 H), 4.15 (t, *J* = 4.0 Hz, 4 H), 4.43

(s, 2 H), 4.49 (s, 4 H), 6.57 (s, 4 H), 7.18–7.24 (m, 3 H), 7.25–7.28 (m, 3 H), 7.29–7.32 (m, 2 H), 7.37–7.46 (m, 6 H), 7.82 (s, 2 H), 7.90 (s, 1 H) ppm. ^{13}C NMR (100 MHz, $CDCl_3$): δ = 18.3, 31.5, 57.8, 58.9, 66.5, 68.5, 68.8, 69.5, 70.0, 70.3, 70.4, 70.5, 70.6, 71.8, 72.2, 83.9, 88.2, 107.1, 122.0 (q, J = 288 Hz), 124.9, 126.6, 127.8, 129.4, 129.5, 130.3, 133.2, 138.3, 144.7, 152.7 ppm. ^{19}F NMR (376 MHz, $CDCl_3$): δ = –73.65 ppm. HRMS (MALDI-TOF): calcd. 3130.4673 $[M + Na]^+$; found 3130.3416.

Synthesis of 1c: A solution of I_2 (2.05 g, 8.07 mmol) in CH_2Cl_2 (20 mL) was added to a solution of **14** (25.10 g, 8.07 mmol) in CH_2Cl_2 (50 mL) in portions over 30 min. The mixture was stirred at room temperature for 4 h and was then quenched with 10 % aqueous sodium thiosulfate (20 mL). The mixture was washed with brine, dried with Na_2SO_4, and concentrated under vacuum to provide a pale-yellow oil. Purification by column chromatography (MeOH/CH_2Cl_2 = 1:25) gave desired product **1c** (18.99 g, 82 %) as a pale-yellow oil. ^{1}H NMR (400 MHz, $CDCl_3$): δ = 2.87 (t, J = 4.0 Hz, 4 H), 3.37 (s, 36 H), 3.50–3.57 (m, 25 H), 3.60–3.74 (m, 297 H), 3.82 (t, J = 4.0 Hz, 18 H), 4.08 (t, J = 4.0 Hz, 15 H), 4.14 (t, J = 4.0 Hz, 9 H), 4.44 (s, 4 H), 4.48 (s, 8 H), 6.57 (s, 8 H), 7.81 (s, 4 H), 7.88 (s, 2 H) ppm. ^{13}C NMR (100 MHz, $CDCl_3$): δ = 38.3, 53.6, 58.9, 68.4, 68.8, 69.4, 69.4, 69.6, 70.0, 70.2, 70.26, 70.29, 70.38, 70.44, 70.5, 71.7, 72.1, 83.8, 88.3, 106.9, 122.0 (q, J = 290 Hz), 125.0, 127.4, 129.3, 130.6, 133.2, 137.8, 152.5 ppm. ^{19}F NMR (376 MHz, $CDCl_3$): δ = –73.59 ppm.

Synthesis of 1b: Under an argon atmosphere, PEt_3 (1.02 mL, 6.96 mmol) was added to a solution of **1c** (18.99 g, 3.31 mmol) in THF/H_2O (9:1, 20 mL). The resulting mixture was stirred at room temperature. After 1 h, the organic solvent was removed under reduced pressure. Under an atmosphere of argon, a solution of **1a** (18.98 g, 6.62 mmol) and NaOH (0.53 g, 13.24 mmol) in EtOH (50 mL) was stirred for 10 min at 0 °C. CH_3I (0.82 mL, 13.24 mmol) was then added dropwise to the mixture over a period of 20 min at 0 °C. The mixture was stirred at ambient temperature overnight. The solvent was evaporated under reduced pressure, and the residue was purified by column chromatography (MeOH/CH_2Cl_2 = 1:25) to afford sulfide **1b** as a colorless oil (12.80 g, 67 %). ^{1}H NMR (400 MHz, $CDCl_3$): δ = 2.93 (t, J = 4.0 Hz, 2 H), 3.38 (s, 18 H), 3.52–3.58 (m, 12 H), 3.58–3.69 (m, 130 H), 3.69–3.81 (m, 23 H), 3.83 (t, J = 4.0 Hz, 9 H), 4.10 (t, J = 4.0 Hz, 8 H), 4.14 (t, J = 4.0 Hz, 4 H), 4.39–4.59 (m, 6 H), 6.57 (s, 4 H), 7.72–7.92 (m, 2 H), 8.01 (s, 1 H) ppm. ^{13}C NMR (100 MHz, $CDCl_3$): δ = 5.58, 5.63, 8.7, 15.8, 19.2, 19.8, 30.6, 33.3, 38.2, 46.3, 58.9, 68.3, 68.5, 68.8, 69.5, 69.6, 69.9, 70.15, 70.21, 70.4, 70.6, 70.8, 71.0, 71.2, 71.8, 72.2, 74.6, 82.4, 82.7, 83.8, 88.3, 106.8, 107.1, 114.5, 122.2 (q, J = 288 Hz), 124.9, 126.0, 128.3, 129.4, 130.3, 130.8, 133.2, 136.9, 138.0, 138.2, 152.55, 152.62 ppm.^{19}F NMR (376 MHz, $CDCl_3$): δ = –73.66 ppm. HRMS (MALDI-TOF): calcd. 2902.3734 $[M + Na]^+$; found 2902.2285.

Preparation of 1a-Modified GNPs: To stirring first-grade water (100 mL) was added aqueous trisodium citrate (0.034 M, 6 mL). After the solution had boiled for 3 min, aqueous $HAuCl_4$ (0.024 M, 2 mL) was added rapidly, and the resulting solution was boiled for another 6 min. Then, the mixture was cooled to room temperature, and the solution was stored in the dark at 4 °C. DLS: diameter = 19.56 nm and polydispersity index (PDI) = 0.409. UV/Vis: V_{max} = 518.50 nm. Under an argon atmosphere, a solution of **1a** (0.20 g, 0.07 mmol) in MeOH (10 mL) was added to the solution of colloidal gold nanoparticles (GNPs), and the mixture was stirred for 24 h at room temperature. The resulting mixture was centrifuged at 16000 ×g for 20 min, and the supernatant was carefully removed. The **1a**-stabilized GNPs were washed with Milli-Q water (3×). The concentration of the functionalized gold nanoparticles was determined by visible absorbance at 525.50 nm. DLS: diameter = 24.33 nm and PDI = 0.306.

Synthesis of 15: A mixture of **5** (61.28 g, 123.90 mmol) and NaN_3 (24.16 g, 371.70 mmol) in dry DMF (600 mL) was stirred at 80 °C for 5 h. The resulting mixture was filtered to remove the excess amount of NaN_3. After removing DMF by vacuum distillation, the residue was washed with water and extracted with CH_2Cl_2 (4 × 300 mL). The organic layers were combined, and the solution was concentrated under vacuum. The residue was purified by column chromatography (EtOAc/petroleum ether = 1:4) to give **15** as a colorless oil (44.37 g, 98 %). ^{1}H NMR (400 MHz, $CDCl_3$): δ = 3.38 (s, 3 H), 3.39–3.43 (m, 2 H), 3.52–3.58 (m, 2 H), 3.63–3.69 (m, 24 H) ppm.

Synthesis of 16: PPh_3 (44.84 g, 170.97 mmol) was added to a stirring solution of **15** (41.65 g, 113.98 mmol) in THF (550 mL) at room temperature. After the addition, the mixture was stirred for 30 min and H_2O (10.27 mL, 569.90 mmol) was added. The resulting mixture was stirred at this temperature overnight. The mixture was extracted with H_2O (2 × 300 mL). The combined aqueous layer was concentrated under vacuum, and the residue was purified by column chromatography (MeOH/CH_2Cl_2 = 1:25) to afford **16** as a colorless oil (36.75 g, 95 %). ^{1}H NMR (400 MHz, $CDCl_3$): δ = 3.39 (s, 3 H), 3.53–3.59 (m, 2 H), 3.60–4.08 (m, 26 H) ppm.

Synthesis of 17: Under an argon atmosphere, a solution of **16** (36.75 g, 108.27 mmol), DMAP (0.66 g, 5.41 mmol), and Et_3N (13.15 g, 129.92 mmol) in dry CH_2Cl_2 (300 mL) was stirred for 10 min at 0 °C. Bromoacetyl bromide (18.84 mL, 216.54 mmol) was then added dropwise to the mixture over a period of 30 min at 0 °C. The mixture was stirred at ambient temperature overnight. The solvent was evaporated under reduced pressure, and then ethyl acetate was added for dissolution. The resulting mixture was filtered to remove a white insoluble solid, and the residue was purified by column chromatography (CH_2Cl_2) to afford **17** as a pale-yellow oil (30.90 g, 62 %). ^{1}H NMR (400 MHz, $CDCl_3$): δ = 3.38 (s, 3 H), 3.45–3.62 (m, 6 H), 3.62–3.72 (m, 22 H), 3.88 (s, 1 H), 4.06 (s, 1 H) ppm. ^{13}C NMR (100 MHz, $CDCl_3$): δ = 29.0, 39.5, 39.8, 42.5, 58.8, 69.2, 70.1, 70.3, 70.4, 71.7, 166.2 ppm. HRMS (ESI): calcd. for $C_{17}H_{34}BrNaNO_8^+$ $[M + Na]^+$ 482.1360; found 482.1352.

Synthesis of 18: Under an argon atmosphere, a solution of benzylamine (3.27 g, 30.51 mmol), **17** (30.90 g, 67.12 mmol), and K_2CO_3 (6.33 g, 45.76 mmol) in dry THF/DMF (1:1, 200 mL) was stirred at 45 °C overnight. DMF was removed by vacuum distillation, and the residue was washed with water and extracted with CH_2Cl_2 (4 × 200 mL). The organic layers were combined, and the solution was concentrated under vacuum. The residue was purified by column chromatography (MeOH/CH_2Cl_2 = 1:50) to give **18** as a colorless oil (24.57 g, 93 %). ^{1}H NMR (400 MHz, $CDCl_3$): δ = 3.21 (s, 4 H), 3.38 (s, 6 H), 3.42–3.51 (m, 4 H), 3.52–3.58 (m, 8 H), 3.58–3.69 (m, 45 H), 3.73 (s, 2 H), 7.27–7.33 (m, 2 H), 7.34–7.37 (m, 3 H) ppm. ^{13}C NMR (100 MHz, $CDCl_3$): δ = 38.8, 57.8, 58.9, 59.2, 69.6, 70.1, 70.36, 70.38, 70.41, 70.45, 71.8, 127.5, 128.4, 129.0, 137.3, 170.4 ppm. HRMS (ESI): calcd. for $C_{41}H_{75}N_3NaO_{16}^+$ $[M + Na]^+$ 888.5040; found 888.5017.

Synthesis of 19: Under a hydrogen atmosphere, a solution of **18** (24.57 g, 28.37 mmol) and Pd/C (4.91 g, 20 % of the mass of **18**) in MeOH (200 mL) was stirred at room temperature overnight. The resulting mixture was filtered to remove Pd/C and was concentrated; then, the residue was purified by column chromatography (MeOH/CH_2Cl_2 = 1:20) to give **19** as a colorless oil (20.25 g, 92 %). ^{1}H NMR (400 MHz, $CDCl_3$): δ = 3.29 (s, 4 H), 3.38 (s, 6 H), 3.44–3.51 (m, 4 H), 3.53–3.60 (m, 8 H), 3.60–3.72 (m, 45 H), 7.52 (t, J = 8.0 Hz, 2 H) ppm. ^{13}C NMR (100 MHz, $CDCl_3$): δ = 38.8, 52.3, 58.8, 69.7, 70.0, 70.3, 71.7, 171.2 ppm. HRMS (ESI): calcd. for $C_{34}H_{70}N_3O_{16}^+$ $[M + H]^+$ 776.4751; found 776.4756.

Synthesis of 20: Compound **20** was prepared by following the same procedure as that outlined for **17** from **16** as a clear oil

(14.51 g, 62 %). ^{1}H NMR (400 MHz, $CDCl_3$): δ = 3.38 (s, 6 H), 3.42–3.51 (m, 4 H), 3.53–3.60 (m, 8 H), 3.61–3.73 (m, 46 H), 4.01–4.19 (m, 6 H) ppm. ^{13}C NMR (100 MHz, $CDCl_3$): δ = 39.4, 39.5, 41.0, 53.5, 54.0, 59.0, 69.2, 69.4, 70.1, 70.2, 70.4, 70.47, 70.53, 71.9, 167.8, 168.5, 169.0 ppm. HRMS (ESI): calcd. for $C_{36}H_{72}BrN_3O_{17}^{2+}$ $[M + 2H]^{2+}$ 448.7017; found 448.7082.

Synthesis of 21: Compound **21** was prepared by following the same procedure as that outlined for **14** from **13** as a clear oil (12.28 g, 90 %). ^{1}H NMR (400 MHz, $CDCl_3$): δ = 2.40 (t, J = 8.0 Hz, 2 H), 3.27 (t, J = 8.0 Hz, 2 H), 3.35 (s, 12 H), 3.39–3.48 (m, 10 H), 3.49–3.83 (m, 116 H), 3.98 (s, 4 H), 4.06 (s, 4 H), 4.27 (s, 4 H), 4.40 (s, 2 H), 7.13–7.24 (m, 6 H), 7.26–7.31 (m, 2 H), 7.36–7.43 (m, 6 H), 7.72 (s, 2 H), 7.97–8.11 (m, 3 H), 9.35 (s, 2 H) ppm. ^{13}C NMR (100 MHz, $CDCl_3$): δ = 31.5, 39.2, 39.3, 52.9, 53.1, 53.7, 58.7, 64.9, 66.3, 68.9, 69.3, 69.4, 69.9, 70.0, 70.2, 70.29, 70.30, 71.7, 82.5, 82.8, 83.1, 83.6, 88.5, 121.7 (q, J = 288 Hz), 125.1, 126.5, 127.7, 129.0, 129.4, 129.9, 133.1, 144.6, 167.1, 168.7, 169.3 ppm. ^{19}F NMR (376 MHz, $CDCl_3$): δ = –74.20 ppm. HRMS (ESI): calcd. for $C_{114}H_{176}F_{12}N_6Na_2O_{40}S^{2+}$ $[M + 2Na]^{2+}$ 1287.5618; found 1287.5597.

Synthesis of 2c: Compound **2c** was prepared by following the same procedure as that outlined for **1c** from **13** as a clear oil (9.18 g, 80 %). ^{1}H NMR (400 MHz, $CDCl_3$): δ = 2.88 (t, J = 4.0 Hz, 4 H), 3.38 (s, 24 H), 3.42–3.84 (m, 256 H), 4.00 (s, 8 H), 4.09 (s, 8 H), 4.29 (s, 8 H), 4.45 (s, 4 H), 7.75 (s, 4 H), 8.06 (s, 6 H), 9.41 (s, 4 H) ppm. ^{13}C NMR (100 MHz, $CDCl_3$): δ = 38.2, 39.2, 39.3, 52.8, 53.0, 58.77, 58.81, 64.9, 69.0, 69.4, 70.0, 70.3, 70.4, 71.69, 71.71, 82.4, 82.7, 83.0, 83.7, 88.3, 121.7 (q, J = 287 Hz), 125.1, 127.7, 129.0, 133.2, 167.2, 168.6, 169.2 ppm. ^{19}F NMR (376 MHz, $CDCl_3$): δ = –74.39 ppm.

Synthesis of 2b: Compound **2b** was prepared by following the same procedure as that outlined for **1b** from **1c** as a clear oil (5.89 g, 65 %). ^{1}H NMR (400 MHz, $CDCl_3$): δ = 2.14 (s, 3 H), 2.70 (t, J = 8.0 Hz, 2 H), 3.38 (s, 12 H), 3.52–3.81 (m, 128 H), 4.01 (s, 4 H), 4.08 (s, 4 H), 4.29 (s, 4 H), 4.45 (s, 2 H), 7.76 (s, 2 H), 8.02 (s, 1 H) ppm. ^{13}C NMR (100 MHz, $CDCl_3$): δ = 14.0, 15.8, 22.6, 26.9, 29.2, 29.5, 29.9, 31.8, 33.3, 36.9, 39.2, 39.3, 53.1, 53.3, 53.6, 58.8, 65.1, 68.9, 69.5, 70.1, 70.2, 70.4, 71.8, 82.9, 83.7, 88.4, 121.7 (q, J = 286 Hz), 125.2, 126.5, 127.7, 129.0, 129.5, 133.2, 144.7, 167.2, 168.7, 169.3 ppm. ^{19}F NMR (376 MHz, $CDCl_3$): δ = –73.93 ppm. HRMS (ESI): calcd. for $C_{96}H_{168}F_{12}N_7Na_2O_{40}S^{3+}$ $[M + 2Na + NH_4]^{3+}$ 788.3545; found 788.3533.

Preparation of 2a-Modified GNPs: To stirring first-grade water (100 mL) was added aqueous trisodium citrate (0.034 M, 8 mL). After the solution had boiled for 3 min, aqueous $HAuCl_4$ (0.024 M, 2 mL) was added rapidly, and the resulting solution was boiled for another 6 min. Then, the mixture was cooled to room temperature, and the solution was stored in the dark at 4 °C. DLS: diameter = 21.51 nm and PDI = 0.320. UV/Vis: V_{max} = 519.50 nm. Under an argon atmosphere, a solution of **2a** (0.20 g, 0.07 mmol) in MeOH (10 mL) was added to the solution of the GNPs, and the mixture was stirred for 24 h at room temperature. The resulting mixture was centrifuged at 16000 ×g for 20 min, and the supernatant was carefully removed. The **2a**-stabilized GNPs were washed with Milli-Q water (3×). The concentration of the functionalized gold nanoparticles was determined by visible absorbance at 527.00 nm. DLS: diameter = 21.94 nm and PDI = 0.131.

Acknowledgments

We are thankful for financial support from the National Key Research and Development Program of China (2016YFC1304704), the National Natural Science Foundation of China (21372181, 21402144 and 21572168), State Key Laboratory for Magnetic Resonance and Atomic and Molecular Physics (Wuhan Institute of Physics and Mathematics), and State Key Laboratory for Modification of Chemical Fibers and Polymer Materials (Donghua University).

Keywords: Self-assembly · Drug delivery · Fluorine · Dendrimers · Stacking interactions

[1] For recent reviews, see: a) G. Gauchervieve, M.-H. Dufresne, V. O. Sant, N. Kang, D. Maysinger, J.-C. Leroux, *J. Controlled Release* **2005**, *109*, 169–188; b) M. Ding, J. Li, H. Tan, Q. Fu, *Soft Matter* **2012**, *8*, 5414–5428; c) Z. Ge, S. Liu, *Chem. Soc. Rev.* **2013**, *42*, 7289–7325; d) W. Cui, J. Li, G. Decher, *Adv. Mater.* **2016**, *28*, 1302–1311.

[2] Y. Jin, R. W. Molt Jr., J. P. Waltho, N. G. Richards, G. M. Blackburn, *Angew. Chem. Int. Ed.* **2016**, *55*, 3318–3322; *Angew. Chem.* **2016**, *128*, 3379–3383.

[3] a) C. T. Gee, E. J. Koleshi, W. C. K. Pomerantz, *Angew. Chem. Int. Ed.* **2015**, *54*, 3735–3739; *Angew. Chem.* **2015**, *127*, 3806–3810; b) N. G. Sharaf, R. Ishima, A. M. Gronenborn, *Biochemistry* **2016**, *55*, 3864–3873.

[4] a) Y. Ye, X. Liu, G. Xu, M. Liu, C. Li, *Angew. Chem. Int. Ed.* **2015**, *54*, 5328–5330; *Angew. Chem.* **2015**, *127*, 5418–5420; b) M. Sarker, K. E. Orrell, L. Xu, M.-L. Tremblay, J. J. Bak, X.-Q. Liu, J. K. Rainey, *Biochemistry* **2016**, *55*, 3048–3059.

[5] G. Sicilia, A. L. Davis, S. G. Spain, J. P. Magnusson, N. R. B. Boase, K. J. Thurecht, C. Alexander, *Polym. Chem.* **2016**, *7*, 2180–2191.

[6] a) E. T. Ahrens, R. Flores, H. Xu, P. A. Morel, *Nat. Biotechnol.* **2005**, *23*, 983–987; b) J. M. Janjic, M. Srinivas, D. K. Kadayakkara, E. T. Ahrens, *J. Am. Chem. Soc.* **2008**, *130*, 2832–2841; c) D. Vivian, K. Cheng, S. Khuranan, S. Xu, E. H. Kriel, P. A. Dawson, J. P. Raufman, J. E. Polli, *Mol. Pharm.* **2014**, *11*, 1575–1582; d) Z.-X. Jiang, X. Liu, E. K. Jeong, Y. B. Yu, *Angew. Chem. Int. Ed.* **2009**, *48*, 4755–4758; *Angew. Chem.* **2009**, *121*, 4849–4852.

[7] Y. Takaoka, K. Kiminami, K. Mizusawa, K. Matsuo, M. Narazaki, T. Matsuda, I. Hamachi, *J. Am. Chem. Soc.* **2011**, *133*, 11725–11731.

[8] Y. B. Yu, *Nanomed. Nanobiotech.* **2013**, *5*, 646–661.

[9] a) M. B. Taraban, Y. Li, F. Yue, E. V. Jouravleva, M. A. Anisimov, Z.-X. Jiang, Y. B. Yu, *RSC Adv.* **2014**, *4*, 54565–54575; b) J. M. Criscione, B. L. Le, E. Stern, M. Brennan, C. Rahner, X. Papademetris, T. M. Fahmy, *Biomaterials* **2009**, *30*, 3946–3955.

[10] a) S. Bo, C. Song, Y. Li, W. Yu, S. Chen, X. Zhou, Z. Yang, X. Zheng, Z.-X. Jiang, *J. Org. Chem.* **2015**, *80*, 6360–6366; b) W. Yu, Y. Yang, S. Bo, Y. Li, S. Chen, Z. Yang, X. Zheng, Z.-X. Jiang, X. Zhou, *J. Org. Chem.* **2015**, *80*, 4443–4447.

[11] H. Zhang, X. Li, Q. Shi, Y. Li, G. Xia, L. Chen, Z. Yang, Z.-X. Jiang, *Angew. Chem. Int. Ed.* **2015**, *54*, 3763–3767; *Angew. Chem.* **2015**, *127*, 3834–3838.

[12] a) C. Gentilini, F. Evangelista, P. Rudolf, P. Franchi, M. Lucarini, L. Pasquato, *J. Am. Chem. Soc.* **2008**, *130*, 15678–15682; b) M. Boccalon, P. Franchi, M. Lucarini, J. J. Delgado, F. Sousa, F. Stellacci, I. Zucca, A. Scotti, R. Spreafico, P. Pengo, L. Pasquato, *Chem. Commun.* **2013**, *49*, 8794–8796; c) O. Michelena, D. Padro, C. Carrillo-Carrion, P. del Pino, J. Blanco, B. Arnaiz, W. J. Parak, M. Carril, *Chem. Commun.* **2017**, *53*, 2447–2450.

Received: April 24, 2017

